Anisotropy in breakdown field of 4H–SiC

Shun-ichi Nakamura,[a] Hironori Kumagai, Tsunenobu Kimoto, and Hiroyuki Matsunami
Department of Electronic Science and Engineering, Kyoto University, Yoshidahonmachi, Sakyo, Kyoto 606-8501, Japan

(Received 4 January 2002; accepted for publication 12 March 2002)

The breakdown fields along the $\langle 11\bar{2}0\rangle$ and $\langle 03\bar{3}8\rangle$ directions in 4H–SiC have been measured. For the measurements, epitaxial p^+n diodes with mesa structures were fabricated on the $(11\bar{2}0)$ and $(03\bar{3}8)$ faces, and they showed good rectification properties and avalanche breakdown. The breakdown fields along these directions calculated from the breakdown voltage were found to be about three quarters of that along the $\langle 0001\rangle$ direction in 4H–SiC. The cause of the anisotropy in breakdown field is discussed. © *2002 American Institute of Physics.* [DOI: 10.1063/1.1477271]

Silicon carbide (SiC) is one of the most promising semiconductor materials for power devices, owing to its superior electrical and thermal properties. In particular, breakdown field and impact ionization coefficients are the most important material properties in designing power devices. The breakdown fields[1–3] as well as the impact ionization coefficients[4,5] along the $\langle 0001\rangle$ direction in both 6H– and 4H–SiC have been reported, and it was found that the impact ionization coefficient of holes along the $\langle 0001\rangle$ direction is much larger than that of electrons, as contrasted with most of other common semiconductor materials. It was also reported that the breakdown field in 6H–SiC shows strong anisotropy:[1] the breakdown field along the direction perpendicular to the $\langle 0001\rangle$ direction is about two thirds of that along the $\langle 0001\rangle$ direction. However, the anisotropy of breakdown field in 4H–SiC, a more attractive polytype for power devices, has not been reported. Recently, it was suggested that the use of other faces than (0001) in 4H–SiC, namely $(11\bar{2}0)$ (Ref. 6) and $(03\bar{3}8)$ (Ref. 7), may improve the performance of metal–oxide–semiconductor devices, and the breakdown fields along the directions perpendicular to these faces have emerged as critical issues. Even in 4H–SiC devices on off-axis (0001), the anisotropy in the breakdown field is an important property to design device structures, because the electric field distribution is always three-dimensional. In this letter, the breakdown fields along these directions are measured.

To measure the breakdown field, epitaxial p^+n diodes were fabricated. By employing a mesa structure, we can assume parallel-plane breakdown, when the mesa is high enough for the depletion region not to reach the bottom of mesa. The substrates used in this work were heavily doped (more than 10^{18} cm^{-3}) n-type 4H–SiC (0001) faces inclined by 8° toward $\langle 11\bar{2}0\rangle$, and on-axis $(11\bar{2}0)$ and $(03\bar{3}8)$ faces. The epilayers were grown simultaneously in a horizontal cold-wall chemical vapor deposition reactor[8] using SiH_4 and C_3H_8 as source gases and H_2 as a carrier gas. Nitrogen and trimethylaluminum were used as doping sources for n and p^+ layers, respectively. The designed doping concentration for the n layer and the mesa height are summarized in Table I. The diameter of mesa was 60 or 100 μm. The p^+ layer actually consists of two parts: the first layer (adjacent to the n-layer) is a 1.3 μm-thick anode layer with an acceptor concentration of about 1×10^{18} cm^{-3}, and the second layer is a 0.4 μm-thick contact layer, in which the acceptor concentration is much higher than the anode, in order to reduce the contact resistance. The mesa structure was formed by reactive ion etching using CF_4 and O_2, and then passivated by thermal oxides grown at 1150 °C for 1 h in a wet ambient and annealed at the same temperature for 30 min in an argon ambient. Ohmic contacts for the substrates and p^+ contact layer were nickel and titanium covered with aluminum, respectively, sintered at 800 °C for 10 min in an argon ambient.

The growth condition for the designed doping concentration was determined for 4H–SiC (0001), and the mesa height was designed to be larger than the maximum depletion width calculated from the breakdown field along 4H–SiC $\langle 0001\rangle$ previously suggested by another group.[4] In general, more nitrogen atoms are incorporated into other faces than (0001),[9] which should not cause a premature breakdown at the bottom of mesa; because the higher the donor concentration is, the thinner the maximum depletion width is. However, an attention has to be paid to the fact that less aluminum atoms are incorporated into other faces than (0001).[9] From the growth conditions,[9] the acceptor concentrations in the p anodes are estimated to be 1×10^{18} cm^{-3}, 5×10^{17} cm^{-3}, and 7.5×10^{17} cm^{-3} for (0001), $(11\bar{2}0)$, and $(03\bar{3}8)$, respectively, which are not much higher than the donor concentrations.

For an abrupt but not one-sided $p-n$ junction, where the acceptor concentration in the p layer, N_a, is not much higher than the donor concentration in the n layer, N_d, the depletion region extends to both of the n and p layers. Hence, from

TABLE I. The designed donor concentration and device parameter of the n layer of fabricated diodes. The donor concentration is designed for 4H–SiC (0001).

Structure	N_d (cm^{-3})[a]	h (μm)[b]
1	1×10^{16}	14
2	1×10^{17}	2
3	4×10^{17}	10

[a]Donor concentration of the n layer.
[b]Mesa height excluding the p^+ layer.

[a]Electronic mail: syu-naka@kuee.kyoto-u.ac.jp

0003-6951/2002/80(18)/3355/3/$19.00 © 2002 American Institute of Physics
Downloaded 24 Dec 2006 to 130.54.130.229. Redistribution subject to AIP license or copyright, see http://apl.aip.org/apl/copyright.jsp

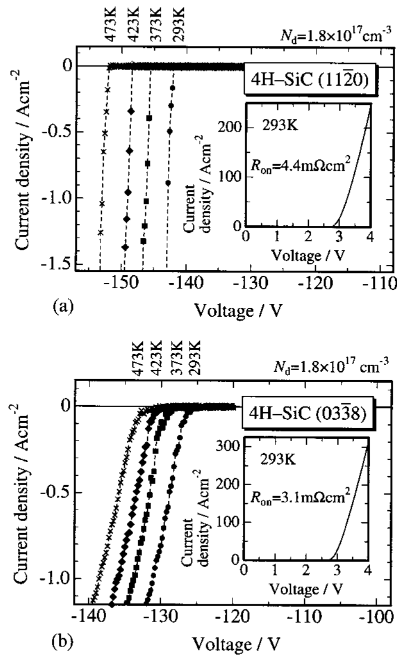

FIG. 1. Typical reverse current–voltage ($I-V$) characteristics of diodes fabricated on (a) 4H–SiC $(11\bar{2}0)$ and (b) 4H–SiC $(03\bar{3}8)$ measured at room and elevated temperatures. Insets show forward $I-V$ characteristics measured at room temperature.

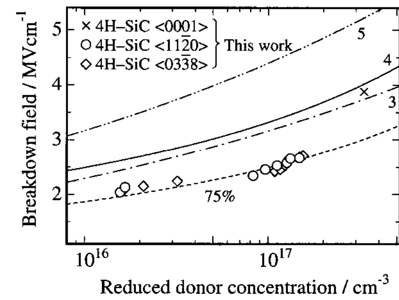

FIG. 2. Breakdown fields along 4H–SiC $\langle 11\bar{2}0\rangle$, and $\langle 03\bar{3}8\rangle$ obtained in this work. Open circles and diamonds stand for the breakdown field along $\langle 11\bar{2}0\rangle$ and $\langle 03\bar{3}8\rangle$, respectively. Curves marked as 3, 4, and 5 are the breakdown fields along 4H–SiC $\langle 0001\rangle$ (suggested by Refs. 3, 4, and 5, respectively). The curve indicated as 75% denotes the 75% of the value (previously suggested in Ref. 4).

capacitance–voltage $(C-V)$ measurements, the "reduced donor concentration" N_B is obtained, as N_d is for an one-sided p^+n junction. N_B is expressed as $N_aN_d(N_a+N_d)^{-1}$, and approaches N_d when N_a is much higher than N_d. The maximum electric field at breakdown, which we define the breakdown field, is given as $\sqrt{2e(V_d+|V_B|)N_B\varepsilon_{\mathrm{SiC}}{}^{-1}}$, where e, $\varepsilon_{\mathrm{SiC}}$, and V_B are the magnitude of electronic charge, the permittivity of SiC, and the breakdown voltage, respectively. V_d is the built-in potential, to which we applied the value obtained from the $C-V$ measurements.

The breakdown measurements were done with a protective resistance $(100\ \mathrm{k}\Omega)$ in series, and by applying a step voltage with a step width of 416 μs, which is short enough to be considered as a pulse operation. The breakdown voltage is defined as the intercept on the voltage axis of the line extrapolated from the region where the reverse current linearly increases with increasing reverse voltage.

Figure 1 shows the typical electrical properties of the diodes fabricated on 4H–SiC $(11\bar{2}0)$ and $(03\bar{3}8)$. The diodes show good rectification properties. The specific on resistances R_{on} were below 10 $\mathrm{m}\Omega\,\mathrm{cm}^2$, implying that parasitic resistances are negligible in determining the breakdown voltage. For $(03\bar{3}8)$, the onset of breakdown is rather gentle and seems like soft breakdown. This may be attributed to relatively poor crystallinity of $(03\bar{3}8)$ wafers currently available. The breakdown voltages for both $(11\bar{2}0)$ and $(03\bar{3}8)$ clearly increase with increasing temperature, suggesting avalanche breakdown. The calculated breakdown field also showed positive temperature coefficients of 6×10^2 and 4×10^2 V/cm K for $(11\bar{2}0)$ and $(03\bar{3}8)$, respectively. The diodes with structures 1 and 2 simultaneously fabricated on (0001) did not show reasonable breakdown voltages because the donor concentrations were accidentally so low as to extend the depletion layers beyond the bottom of mesa. However, the diodes with structure 3 agreed well with the breakdown field previously reported,[3,4] and showed positive but smaller temperature coefficients $(2\times10^2$ V/cm K).

Figure 2 shows the breakdown fields at room temperature along 4H–SiC $\langle 11\bar{2}0\rangle$ and $\langle 03\bar{3}8\rangle$ obtained in this work, and that along 4H–SiC $\langle 0001\rangle$ suggested by literatures.[3–5] The breakdown fields along 4H–SiC $\langle 11\bar{2}0\rangle$ and $\langle 03\bar{3}8\rangle$ were found to be about three quarters of that along 4H–SiC $\langle 0001\rangle$ reported.[3,4]

For 6H–SiC, it was reported[1] that the breakdown field along $\langle 0001\rangle$ is larger than that along the direction perpendicular to $\langle 0001\rangle$, because the impact ionzation coefficient of electrons along $\langle 0001\rangle$ is much smaller than that along the perpendicular direction, while those of holes are not very different. Similarly, the larger breakdown field along $\langle 0001\rangle$ in 4H–SiC should be attributed to the smaller impact ionization coefficient of electrons only along $\langle 0001\rangle$, explained as follows. In 4H–SiC and many other common polytypes of SiC except for 3C–SiC, the conduction band is split into minibands within the first Brillouin zone only along the $\langle 0001\rangle$ direction.[10] The conduction band splitting comes from the long period along $\langle 0001\rangle$ just like splitting in phonon dispersion curve,[11,12] but far stronger interactions between electron waves cause much wider splitting between the minibands. Assuming sinusoidal potential by the long period and the same potential from core electrons as in 3C–SiC, one-dimensional Schrödinger's equation has been solved to estimate the miniband structure.[13] The conduction band splitting between the first and second minibands in 4H–SiC along $\langle 0001\rangle$ was estimated[13] to be about 1 eV as shown in Fig. 3, which is large enough to assume very few electrons in the higher miniband at thermal equilibrium. In addition, the conduction band splitting is large enough to neglect the Zener tunneling[14,15] of electrons between the first and second minibands under a strong electric field.[16] The splitting in the conduction band also prohibits the electrons in the first miniband to have enough energy to cause impact ionization: in the case of 4H–SiC, electrons in the first miniband can be accelerated to at most 1 eV along $\langle 0001\rangle$.[13] Scattering into higher minibands by either phonons, crystal imperfections, or electrons themselves, is required for the electrons in the first miniband to be accelerated to cause impact ionization, when the electrons can be accelerated only along the $\langle 0001\rangle$ direction. Because the phonon energy is 120 meV or below,[12] many scattering processes (not along $\langle 0001\rangle$) have to occur

Downloaded 24 Dec 2006 to 130.54.130.229. Redistribution subject to AIP license or copyright, see http://apl.aip.org/apl/copyright.jsp

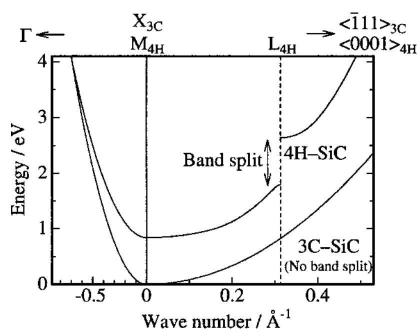

FIG. 3. Schematic conduction band in 4H– and 3C–SiC along ⟨0001⟩ (right-hand side half) (suggested in Ref. 13) and along a direction perpendicular to ⟨0001⟩ (left-hand side half). The wave number is from the conduction band minima (the *M* and *X* points for 4H– and 3C–SiC, respectively). The conduction band in 4H–SiC along ⟨0001⟩ is actually folded at the *L* point.

in a very short period. Scattering by electrons themselves has been neglected in other materials due to its small probability. Therefore, the impact ionization by electrons along ⟨0001⟩ is greatly suppressed. If the ionization coefficient of electrons along a direction is small, the breakdown field along the direction should be consequently large.

The conduction band splitting is not present along the directions perpendicular to ⟨0001⟩ as shown in Fig. 3, and thus the breakdown field along ⟨0001⟩ should be larger than those along $\langle 11\bar{2}0\rangle$ and $\langle 01\bar{1}0\rangle$. For an intermediate direction, the breakdown field should probably take an intermediate value between those along the ⟨0001⟩ direction and along the direction perpendicular to ⟨0001⟩, for example, $\langle 03\bar{3}8\rangle$ is between ⟨0001⟩ and $\langle 01\bar{1}0\rangle$. However, as shown in Fig. 2, the breakdown fields along $\langle 03\bar{3}8\rangle$ and $\langle 11\bar{2}0\rangle$ are almost the same. This is possibly attributed to the lower breakdown field along $\langle 01\bar{1}0\rangle$ than along $\langle 11\bar{2}0\rangle$ (not confirmed yet).

In summary, the breakdown fields along the $\langle 11\bar{2}0\rangle$ and $\langle 03\bar{3}8\rangle$ directions in 4H–SiC have been measured using epitaxial p^+n diodes with mesa structures. They showed good rectification properties and avalanche breakdown. The breakdown fields along these directions calculated from the breakdown voltage were found to be about three quarters of that along the ⟨0001⟩ direction in 4H–SiC. The cause of the anisotropy in the breakdown field can be explained by the split of the conduction band only along the ⟨0001⟩ direction.

This work is partly supported by a Grant-in-Aid for Specially Promoted Research, Grant No. 09102009, by the Ministry of Education, Culture, Sports, Science, and Technology in Japan, and by Feasibility Study of Japan Society for the Promotion of Science. The authors would like to thank SiXON Ltd. for supplying 4H–SiC $(03\bar{3}8)$ substrates.

[1] A. P. Dmitriev, A. O. Konstantinov, D. P. Litvin, and V. I. Sankin, Fiz. Tekh. Poluprovodn. (S.-Peterburg) **17**, 1093 (1983). [Sov. Phys. Semicond. **17**, 686 (1983).]
[2] J. A. Edmond, D. G. Waltz, S. Brueckner, H. S. Kong, J. W. Palmour, and C. H. Carter, Jr., *Proceedings of the First International High Temperature Electronics Conference* 1991, p. 505.
[3] J. W. Palmour, C. H. Carter, Jr., C. E. Weitzel, and K. J. Nordquist, Mater. Res. Soc. Symp. Proc. **339**, 133 (1994).
[4] A. O. Konstantinov, Q. Wahab, N. Nordell, and L. Lindefelt, J. Electron. Mater. **27**, 335 (1998).
[5] R. Raghunathan and B. J. Baliga, Solid-State Electron. **43**, 199 (1999).
[6] H. Yano, T. Hirao, T. Kimoto, H. Matsunami, K. Asano, and Y. Sugawara, IEEE Electron Device Lett. **20**, 611 (1999).
[7] T. Hirao, H. Yano, T. Kimoto, H. Matsunami, and H. Shiomi, Mater. Sci. Forum. **389**, 1065 (2002).
[8] H. Matsunami and T. Kimoto, Mater. Sci. Eng., R. **20**, 125 (1997).
[9] T. Yamamoto, T. Kimoto, and H. Matsunami, Mater. Sci. Forum **264**, 111 (1998).
[10] L. V. Keldysh, Fiz. Tverd. Tela (Leningrad) **4**, 2265 (1962). [Sov. Phys. Solid State **4**, 1658 (1963).]
[11] D. W. Feldman, J. H. Parker, Jr., W. J. Choyke, and L. Patrick, Phys. Rev. **170**, 698 (1968).
[12] D. W. Feldman, J. H. Parker, Jr., W. J. Choyke, and L. Patrick, Phys. Rev. **173**, 787 (1968).
[13] G. B. Dubrovskii, Fiz. Tverd. Tela (Leningrad) **13**, 2505 (1971). [Sov. Phys. Solid State **13**, 2107 (1972).]
[14] J. B. Krieger and G. J. Iafrate, Phys. Rev. B **33**, 5494 (1986).
[15] A. Sibille, Solid-State Electron. **32**, 1455 (1989).
[16] Assuming a triangular potential barrier with 1 eV in height, the barrier width under 1 MV/cm of electric field is 100 Å, which is large enough to neglect tunneling of electrons through the potential barrier.

Downloaded 24 Dec 2006 to 130.54.130.229. Redistribution subject to AIP license or copyright, see http://apl.aip.org/apl/copyright.jsp